JOURNAL OF GUIDANCE, CONTROL, AND DYNAMICS
Vol. 21, No. 3, May–June 1998

Stability Analysis of a Missile Control System with a Dynamic Inversion Controller

Corey Schumacher*
U.S. Air Force Research Laboratory, Wright–Patterson Air Force Base, Ohio 45433-7531
and
Pramod P. Khargonekar†
University of Michigan, Ann Arbor, Michigan 48109-2122

The closed-loop stability is examined of a bank-to-turn, air-to-air missile with a dynamic inversion controller using a two-timescale separation. A state-space formulation for the α, β, and ϕ dynamics of the missile, assuming the inner-loop dynamic inversion is performed exactly, is presented. It is then shown that, under certain assumptions, the exponential stability of the α, β, and ϕ dynamics about the commanded values can be guaranteed if the inner-loop design frequency is large enough. An example calculation of the required inner-loop frequency to guarantee stability is done for a particular bank-to-turn missile. Finally, nonlinear six-degree-of-freedom simulation results of a maneuver performed with the dynamic inversion controller are presented.

Nomenclature

g	= acceleration due to gravity
I_{xx}, I_{yy}, I_{zz}	= moments of inertia about body axes x, y, and z
I_{xz}	= product of inertia about body axes x and z
L, M, N	= aerodynamic rolling, pitching, and yawing moments
m	= missile mass
p, q, r	= roll, pitch, and yaw rates about the body axes
T	= engine thrust force (along the missile body x axis)
V	= missile speed
X, Y, Z	= aerodynamic forces along the body axes x, y, and z
α, β	= angle of attack, sideslip angle
ϕ, θ, ψ	= missile bank (roll) angle, pitch attitude angle, and heading angle

I. Introduction

THIS paper is focused on the theoretical analysis of stability of a closed-loop missile system with a dynamic inversion-based controller. The missile control problem under investigation concerns postboost maneuvering of a bank-to-turn missile. The dynamic inversion controller uses a two-timescale assumption to separate the p, q, r dynamics from the α, β, ϕ dynamics. The outer-loop dynamic inversion for the α, β, ϕ dynamics is performed assuming that the states p, q, r achieve their commanded values instantaneously. This paper examines the stability of the two-timescale dynamic inversion controller when the commanded p, q, r values are not achieved instantaneously.

The bank-to-turn flight of a nonaxisymmetric missile is a highly nonlinear problem. A number of studies have examined the application of dynamic inversion controllers to this type of problem. Background on the application of dynamic inversion controllers to aircraft problems can be found in Refs. 1–5. General background on the stability of nonlinear systems can be found in Refs. 6 and 7.

The paper begins with a brief description of the missile model. These equations of motion for an aircraft, and their derivation, can be found in Refs. 8 and 9. The aerodynamic data used in this study can be found in Ref. 10. The dynamic inversion controller is detailed in Sec. II.B. Next, in Sec. III, we present the main results of this paper. First, we derive a state-space formulation for the α, β, ϕ dynamics, which we will use in our analysis. Then we present and prove the main result of the paper, theorem 2, which states that, under certain (reasonable) assumptions, the closed-loop dynamics with the dynamic inversion controller will be stable about the desired angles of attack, sideslip angle, and roll angle. This result is proven using two related Lyapunov functions. Finally, examples are presented to illustrate some of the key calculations and assumptions.

Received July 28, 1997; revision received Nov. 7, 1997; accepted for publication Nov. 7, 1997. This paper is declared a work of the U.S. Government and is not subject to copyright protection in the United States.

*Research Aerospace Engineer, AFRL/VACC, Building 146, 2210 Eighth Street, Suite 21. E-mail: coreys@falcon.flight.wpafb.af.mil.

†Professor, Department of Electrical Engineering and Computer Science, 1301 Beal Avenue. E-mail: pramod@eecs.umich.edu.

II. Missile Model and Dynamic Inversion Controller

This paper examines the problem of an air-breathing, nonaxisymmetric airframe that is flown in a bank-to-turn mode. In the air-to-air intercept problem, the guidance law produces acceleration commands in the body y and z axes based on estimates of the target motion. These acceleration commands can be converted into commands in roll angle and angle of attack, which are fed into the autopilot. The task of the controller is to track commands in α and ϕ while keeping sideslip angle small. There are many examples of angle-of-attack autopilots in the literature. The reader is referred to Refs. 2, 5, and 11 for treatments of autopilots that control angle of attack.

A. Missile Model

The rigid-body, nonlinear equations of motion for an aircraft of constant mass are[8–10]

$$\dot{\phi} = p + (q \sin\phi + r \cos\phi) \tan\theta \tag{1}$$

$$\dot{\theta} = q \cos\phi - r \sin\phi \tag{2}$$

$$\dot{\psi} = \frac{q \sin\phi + r \cos\phi}{\cos\theta} \tag{3}$$

$$\begin{aligned}\dot{V} = {} & [(T + X)/m] \cos\alpha \cos\beta + (Y/m) \sin\beta \\ & + (Z/m) \sin\alpha \cos\beta + g(-\sin\theta \cos\alpha \cos\beta \\ & + \cos\theta \sin\phi \sin\beta + \cos\theta \cos\phi \sin\alpha \cos\beta)\end{aligned} \tag{4}$$

$$\begin{aligned}\dot{\alpha} = {} & -\frac{T + X}{mV \cos\beta} \sin\alpha + \frac{Z \cos\alpha}{mV \cos\beta} \\ & + q - (p \cos\alpha + r \sin\alpha) \tan\beta \\ & + \frac{g}{V \cos\beta} \cos\alpha \cos\phi \cos\theta \sin\alpha \sin\theta\end{aligned} \tag{5}$$

Table 1 Moments of inertia

$I_{xxzzxz2} = I_{xx} I_{zz} - I_{xz}^2$	$I_{pn} = \dfrac{I_{xz}}{I_{xxzzxz2}}$	$I_{rpq} = \dfrac{I_{xx}(I_{xx} - I_{yy}) + I_{xz}^2}{I_{xxzzxz2}}$
$I_{qm} = \dfrac{1.0}{I_{yy}}$	$I_{rl} = \dfrac{I_{xz}}{I_{xxzzxz2}}$	$I_{qrr} = \dfrac{I_{xz}}{I_{yy}}$
$I_{rn} = \dfrac{I_{xx}}{I_{xxzzxz2}}$	$I_{ppq} = I_{xz} \dfrac{I_{zz} + I_{xx} - I_{yy}}{I_{xxzzxz2}}$	$I_{qpp} = -\dfrac{I_{xz}}{I_{yy}}$
$I_{pqr} = \dfrac{I_{zz}(I_{yy} - I_{zz}) - I_{xz}^2}{I_{xxzzxz2}}$	$I_{rqr} = \dfrac{I_{xz}(I_{yy} - I_{zz}) - I_{xx} I_{xz}}{I_{xxzzxz2}}$	$I_{qpr} = \dfrac{I_{zz} - I_{xx}}{I_{yy}}$

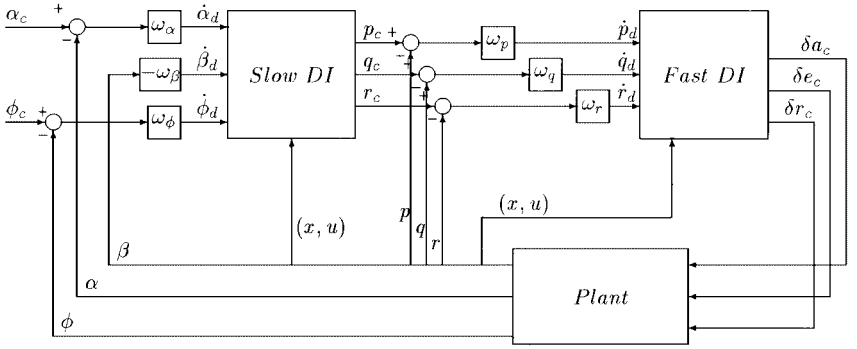

Fig. 1 Dynamic inversion controller structure.

$$\dot{\beta} = -(r\cos\alpha - p\sin\alpha) - \frac{T+X}{mV}\cos\alpha\sin\beta + \frac{Y\cos\beta}{mV} - \frac{Z}{mV}\sin\alpha\sin\beta + \frac{g}{V}(\cos\theta\sin\phi\cos\beta + \sin\theta\cos\alpha\sin\beta - \cos\theta\cos\phi\sin\alpha\sin\beta) \quad (6)$$

$$\dot{p} = I_{ppq}pq + I_{pqr}qr + I_{ppd}p + I_{prd}r + I_{pl}L + I_{pn}N \quad (7)$$

$$\dot{q} = I_{qqd}q + I_{qpp}p^2 + I_{qrr}r^2 + I_{qpr}pr + I_{qm}M \quad (8)$$

$$\dot{r} = I_{rpq}pq + I_{rqr}qr + I_{rpd}p + I_{rrd}r + I_{rl}L + I_{rn}N \quad (9)$$

where the moments of inertia are given in Table 1. The aerodynamic forces and moments are functions of angle of attack, Mach number, sideslip angle, altitude, and control surface deflections.

B. Dynamic Inversion Controller

The design methodology used in this study is a dynamic inversion approach using a two-timescale assumption to separate the dynamics.[1–5,10] The inner-loop inversion uses the control surface deflections to control the fast states p, q, and r. The outer-loop inversion uses the fast states as inputs to control the slow states α, β, and ϕ. The controller structure is shown in Fig. 1.

1. *Dynamic Inversion: Inner-Control Loop for the Fast States*

The inner loop of the dynamic inversion control law controls the fast states p, q, and r. This loop calculates control surface deflection commands from the rate commands p_c, q_c, and r_c given by the slow inversion in Fig. 1. The desired dynamics used are given by $\dot{p}_d = \omega_p(p_c - p)$, $\dot{q}_d = \omega_q(q_c - q)$, and $\dot{r}_d = \omega_r(r_c - r)$, where ω_p, ω_q, and ω_r are design parameters. For the purpose of the fast inversion, the aerodynamic moments L, M, and N are assumed to be functions of δe, δa, and δr. Dimensional aerodynamic derivatives are calculated using a difference approximation about the present states and control positions so that the equations of motion can be made affine in the controls. Then L_0 is the roll moment due to the missile body and is a function of α, β, and Mach number; $L_{\delta a}$ is the roll moment generated per unit aileron deflection; and the other terms in Eq. (11), given subsequently, are similarly defined. The fast inversion equations then become

$$\begin{bmatrix} \delta a_c \\ \delta e_c \\ \delta r_c \end{bmatrix} = [M_1] \times \begin{bmatrix} \dot{p}_d - (I_{ppq}pq + I_{pqr}qr + I_{ppd}p + I_{prd}r + I_{pl}L_0 + I_{pn}N_0) \\ \dot{q}_d - \left(I_{qqd}q + I_{qpp}p^2 + I_{qrr}r^2 + I_{qpr}pr + I_{qm}M_0\right) \\ \dot{r}_d - (I_{rpq}pq + I_{rqr}qr + I_{rpd}p + I_{rrd}r + I_{rl}L_0 + I_{rn}N_0) \end{bmatrix} \quad (10)$$

where

$$M_1 = \begin{pmatrix} I_{pl}L_{\delta a} + I_{pn}N_{\delta a} & I_{pl}L_{\delta e} + I_{pn}N_{\delta e} & I_{pl}L_{\delta r} + I_{pn}N_{\delta r} \\ I_{qm}M_{\delta a} & I_{qm}M_{\delta e} & I_{qm}M_{\delta r} \\ I_{rl}L_{\delta a} + I_{rn}N_{\delta a} & I_{rl}L_{\delta e} + I_{rn}N_{\delta e} & I_{rl}L_{\delta r} + I_{rn}N_{\delta r} \end{pmatrix}^{-1} \quad (11)$$

2. *Dynamic Inversion: Outer-Control Loop for the Slow States*

A second inversion is applied to the dynamics of the slow states α, β, and ϕ. The slow inversion assumes that the fast states track their commanded values instantly, ignoring the effects of transient body rate dynamics. The slow inversion equations also assume that control surface deflections have no direct effect on the slow states. The slow inversion attempts to replace the actual α, β, ϕ dynamics with the desired dynamics: $\dot{\alpha}_d = \omega_\alpha(\alpha_c - \alpha)$, $\dot{\beta}_d = -\omega_\beta\beta$, and $\dot{\phi}_d = \omega_\phi(\phi_c - \phi)$, where ω_α, ω_β, and ω_ϕ are chosen by the designer.

With Eqs. (5) and (6) and the external inputs as just described, the slow inversion control law has the form

$$\begin{bmatrix} p_c \\ q_c \\ r_c \end{bmatrix} = [\mathrm{h}]^{-1} \begin{bmatrix} \dot{\alpha}_d + \left(\dfrac{T+X}{mV\cos\beta}\sin\alpha - \dfrac{Z\cos\alpha}{mV\cos\beta} - \dfrac{g}{V\cos\beta}\cos\alpha\cos\phi\cos\theta + \sin\alpha\sin\theta\right) \\ \dot{\beta}_d + \left(\dfrac{T+X}{mV}\cos\alpha\sin\beta - \dfrac{Y\cos\beta}{mV} + \dfrac{Z}{mV}\sin\alpha\sin\beta - \dfrac{g}{V}(\cos\theta\sin\phi\cos\beta + \sin\theta\cos\alpha\sin\beta - \cos\theta\cos\phi\sin\alpha\sin\beta)\right) \\ \dot{\phi}_d \end{bmatrix} \quad (12)$$

where

$$\mathrm{h} = \begin{pmatrix} -\tan\beta\cos\alpha & 1 & -\tan\beta\sin\alpha \\ \sin\alpha & 0 & -\cos\alpha \\ 1 & \sin\phi\tan\theta & \cos\phi\tan\theta \end{pmatrix} \tag{13}$$

III. Stability Analysis Results

The stability analysis presented in this section constitutes the main contribution of this paper. We show that, under certain assumptions, the closed-loop system can be proved to be exponentially stable about the commanded constant values of α, β, and ϕ by making the frequency of the desired dynamics in the inner-loop inversion sufficiently large.

The dynamic inversion controller uses the assumption that the α, β, ϕ dynamics are much slower than the p, q, r dynamics. This assumption of a timescale separation justifies using p, q, and r as control inputs for the α, β, ϕ dynamics. In a singular perturbation analysis of the validity of the two-timescale assumption, it is assumed that p, q, and r instantaneously achieve their commanded values. This work examines the stability of the two-timescale dynamic inversion controller when the commanded p, q, and r values are not achieved instantaneously. Instead, the much weaker assumption will be made that the inner-loop dynamic inversion is performed correctly, which will result in p, q, and r following trajectories defined by their desired dynamics, i.e., $\dot{p} = \dot{p}_d$, and similarly for q and r.

To perform the stability analysis, it is first necessary to formulate the equations of motion in a state-space form. The dynamic inversion equations are used to convert the equations of motion for α, β, and ϕ into a state-space system for the states $x_1 = \alpha - \alpha_c$, $x_2 = \dot{\alpha}$, $x_3 = \beta$, $x_4 = \dot{\beta}$, $x_5 = \phi - \phi_c$, and $x_6 = \dot{\phi}$. Substituting for the control deflections using the fast inversion equations removes the controls from the system. Substituting for p, q, r, p_c, q_c, and r_c using the slow inversion equations and desired dynamics gives a system in α, β, and ϕ and their derivatives only.

The main result regarding the stability of this state-space system is then given as theorem 2. Because of its length, the proof of this theorem is broken up into several parts. First, a Lyapunov function V_1 is proposed for the α and β dynamics of the state-space system. This function is then expanded to the Lyapunov function V_t, for the entire system. Conditions are derived under which the derivatives of these Lyapunov functions along the trajectories of Eqs. (15–20) (given subsequently) are negative definite. Using bounds on the sizes of the states found from level sets of the Lyapunov functions V_1 and V_t, it is shown that these conditions can be satisfied by all $\omega_i \geq \omega_i^*$ for some ω_i^*.

After the proof of the stability theorem, a numerical example will be given in which the method used in the proof of the theorem will be used to find ω_i^* such that exponential stability is assured. Nonlinear six-degree-of-freedom simulation results will be included as further validation of the assumptions made.

A. Derivation of State-Space Equations

The first step of the analysis is to use the dynamic inversion controller to remove the inner-loop dynamics from the system, resulting in a state-space system for $(\alpha, \beta, \phi, \dot{\alpha}, \dot{\beta}, \dot{\phi})$. The following assumptions are used in the analysis.

Assumption 1. Control deflections have no effect on $\dot{\alpha}$, $\dot{\beta}$, and $\dot{\phi}$. This means that control deflections have no contribution to the forces acting on the missile but contribute only to the moments acting on the missile, i.e., $\partial C_i/\partial\delta j = 0, i = X, Y, Z$, and $j = e, a, r$. This assumption is typical of two-timescale missile controllers.

Assumption 2. The missile's flight speed and dynamic pressure are constant, i.e., $\dot{V}$ and $\dot{\bar{q}} = 0$. This assumption is reasonable over the timescale required to make an attitude-change maneuver.

Assumption 3. Thrust and acceleration due to gravity are zero, i.e., $T = 0$ and $g = 0$. Thrust is zero because only postboost flight is being examined. The assumption that $g = 0$ is made in many angle-of-attack autopilots. The acceleration due to gravity would be included in the acceleration command produced by the guidance law, which can then be converted to angle-of-attack and roll angle commands.

Assumption 4. There is exact fast inversion. It is assumed that complete and exact knowledge of the aerodynamic coefficients is available and that the actuators instantaneously achieve commanded control deflections. More concretely, $\dot{p} = \dot{p}_d$, $\dot{q} = \dot{q}_d$, $\dot{r} = \dot{r}_d$, and $\delta e = \delta e_c$, $\delta a = \delta a_c$, $\delta r = \delta r_c$.

Assumption 5. The commanded inputs α_c and ϕ_c are constant.

Let us define $x_1 := \alpha - \alpha_c$, $x_3 := \beta$, $x_5 := \phi - \phi_c$, $x_2 := \dot{\alpha}$, $x_4 := \dot{\beta}$, and $x_6 := \dot{\phi}$. Furthermore, let $\zeta = (\alpha \;\; \beta \;\; \phi)^T$, $\chi = (p \;\; q \;\; r)^T$, and $\eta = (\alpha \;\; \beta \;\; \phi \;\; \theta)^T$. We can then write

$$\dot{\zeta} = f(\zeta) + h(\eta)\chi \tag{14}$$

where

$$f(\zeta) = \begin{pmatrix} f_1 \\ f_2 \\ 0 \end{pmatrix} = \begin{pmatrix} K(-C_x\sin\alpha + C_z\cos\alpha)/\cos(\beta) \\ K(C_y - C_x\cos\alpha\sin\beta - C_z\sin\alpha\sin\beta) \\ 0 \end{pmatrix}$$

$$K = \bar{q}S/mV$$

and $h(\eta)$ is as defined in Eq. (13). The state-space equations of motion used in the stability analysis are given in the next result.

Proposition 1. Suppose assumptions 1–5 hold. Then Eqs. (1), (5), and (6), under the effect of the dynamic inversion controller detailed in Sec. II.B, become, in state-space form,

$$\dot{x_1} = x_2 \tag{15}$$

$$\dot{x_2} = -\omega_i\omega_\alpha x_1 - x_2\left(\omega_i - \frac{\partial f_1}{\partial\alpha}\right) + \frac{\partial f_1}{\partial\beta}x_4 + l_1 \tag{16}$$

$$\dot{x_3} = x_4 \tag{17}$$

$$\dot{x_4} = -\omega_i\omega_\beta x_3 - x_4\left(\omega_i - \frac{\partial f_2}{\partial\beta}\right) + \frac{\partial f_2}{\partial\alpha}x_2 + l_2 \tag{18}$$

$$\dot{x_5} = x_6 \tag{19}$$

$$\dot{x_6} = -\omega_i\omega_\phi x_5 - \omega_i x_6 + l_3 \tag{20}$$

where

$$\begin{aligned} l_1 = \frac{1}{\det(h)}\Big[&-x_4\sec^2\beta\sin\phi\tan\theta(x_2 - f_1) \\ &+ \Big(x_2(-\tan^2\beta\sin\phi\tan\theta - \tan\beta\sin\alpha\cos\phi\tan\theta \\ &+ \tan\beta\cos\alpha) + x_4(\sec^2\beta\sin\alpha \\ &- \sec^2\beta\cos\alpha\cos\phi\tan\theta)\Big)(x_4 - f_2) + \sec^2\beta x_4 x_6\Big] \end{aligned} \tag{21}$$

$$\begin{aligned} l_2 = \frac{1}{\det(h)}[&x_2\sin\phi\tan\theta(x_2 - f_1) \\ &+ x_2(\sin\alpha - \cos\alpha\cos\phi\tan\theta)(x_4 - f_2) - x_2 x_6] \end{aligned} \tag{22}$$

$$\begin{aligned} l_3 = \frac{1}{\det(h)}\Big[&\Big(x_6(-\cos\phi\cos\alpha\tan\theta - \sin\alpha\tan^2\theta) \\ &- \dot{\theta}\sin\phi\sec^2\theta\cos\alpha\Big)(x_2 - f_1) + \Big(x_6(-\tan\beta\cos\alpha\tan^2\theta \\ &+ \cos\phi\tan\theta\sin\phi\tan\beta - \sin\phi\tan\theta) \\ &+ \dot{\theta}(\cos\phi\sec^2\theta + \sin\phi\sec^2\theta\tan\beta\sin\alpha)\Big)(x_4 - f_2) \\ &+ \Big(x_6(\sin\alpha\sin\phi\tan\theta - \tan\beta\cos\phi\tan\theta) \\ &+ \dot{\theta}(-\tan\beta\sin\phi\sec^2\theta - \sin\alpha\cos\phi\sec^2\theta)\Big)x_6\Big] \end{aligned} \tag{23}$$

$$\det(h) = -\cos\alpha - \sin\alpha\cos\phi\tan\theta - \tan\beta\sin\phi\tan\theta \tag{24}$$

Proof. Under assumptions 1–3, Eqs. (1), (5), and (6) become

$$\dot{\phi} = p + (q\sin\phi + r\cos\phi)\tan\theta$$

$$\dot{\alpha} = -\frac{X}{mV\cos\beta}\sin\alpha + \frac{Z\cos\alpha}{mV\cos\beta} + q - (p\cos\alpha + r\sin\alpha)\tan\beta$$

$$\dot{\beta} = -(r\cos\alpha - p\sin\alpha) - \frac{X}{mV}\cos\alpha\sin\beta + \frac{Y\cos\beta}{mV} - \frac{Z}{mV}\sin\alpha\sin\beta$$

Under assumption 4,

$$\begin{pmatrix} p_c \\ q_c \\ r_c \end{pmatrix} = h^{-1}(\eta)\left[\begin{pmatrix} \dot{\alpha}_d \\ \dot{\beta}_d \\ \dot{\phi}_d \end{pmatrix} - f(\zeta)\right] \tag{25}$$

$$\begin{pmatrix} p \\ q \\ r \end{pmatrix} = h^{-1}(\eta)\left[\begin{pmatrix} \dot{\alpha} \\ \dot{\beta} \\ \dot{\phi} \end{pmatrix} - f(\zeta)\right] \tag{26}$$

Recalling that $\zeta = (\alpha\ \beta\ \phi)^T$, $\chi = (p\ q\ r)^T$, and $\eta = (\alpha\ \beta\ \phi\ \theta)^T$ and differentiating Eq. (14) with respect to time gives

$$\ddot{\zeta} = \frac{\partial f}{\partial \zeta}(\dot{\zeta}) + h(\eta)\dot{\chi} + \left[\frac{\partial h_p}{\partial \eta}\dot{\eta} \quad \frac{\partial h_q}{\partial \eta}\dot{\eta} \quad \frac{\partial h_r}{\partial \eta}\dot{\eta}\right]\chi \tag{27}$$

Substituting for $\dot{p}_d$, $\dot{q}_d$, and $\dot{r}_d$, and for p, q, and r from Eq. (26) into Eq. (27) gives

$$\ddot{\zeta} = \frac{\partial f}{\partial \zeta}(\dot{\zeta}) + h(\eta)\begin{bmatrix} \omega_p & 0 & 0 \\ 0 & \omega_q & 0 \\ 0 & 0 & \omega_r \end{bmatrix} h^{-1}(\eta)\{\dot{\zeta}_d - f(\zeta) - [\dot{\zeta} - f(\zeta)]\} + \left[\frac{\partial h_p}{\partial \eta}\dot{\eta} \quad \frac{\partial h_q}{\partial \eta}\dot{\eta} \quad \frac{\partial h_r}{\partial \eta}\dot{\eta}\right]h^{-1}(\eta)[\dot{\zeta} - f(\zeta)] \tag{28}$$

Now, after defining the inner-loop frequency $\omega_i = \omega_p = \omega_q = \omega_r$ and letting

$$M = \left[\frac{\partial h_p}{\partial \eta}\dot{\eta} \quad \frac{\partial h_q}{\partial \eta}\dot{\eta} \quad \frac{\partial h_r}{\partial \eta}\dot{\eta}\right]$$

we have

$$\begin{pmatrix} \ddot{\alpha} \\ \ddot{\beta} \\ \ddot{\phi} \end{pmatrix} + \left[\omega_i I_{3\times 3} - \frac{\partial f}{\partial \zeta}\right]\begin{pmatrix} \dot{\alpha} \\ \dot{\beta} \\ \dot{\phi} \end{pmatrix} + \begin{pmatrix} \omega_i\omega_\alpha\alpha \\ \omega_i\omega_\beta\beta \\ \omega_i\omega_\phi\phi \end{pmatrix} = \begin{pmatrix} \omega_i\omega_\alpha\alpha_c \\ 0 \\ \omega_i\omega_\phi\phi_c \end{pmatrix} + Mh^{-1}(\eta)[\dot{\zeta} - f(\zeta)] \tag{29}$$

Now we define $(l_1\ \ l_2\ \ l_3)^T = Mh^{-1}(\eta)[\dot{\zeta} - f(\zeta)]$. Substituting for $x_1, \ldots, x_6$ as defined in proposition 1 and expanding $Mh^{-1}(\eta)(\dot{\zeta} - f(\zeta))$ gives the state-space equations in proposition 1. □

B. Statement of the Main Result

The following assumptions will be used in proving the main stability result.

Assumption 6. The commanded angle of attack is that α for which $f_1(\alpha = \alpha_c, \beta = 0) = 0$. For the missile used in this study, this α is 0.8 deg. This is the α at which the missile can hold $\dot{\alpha} = 0$ and $\dot{q} = 0$ at the same time with $\phi = 0$.

Assumption 7. The magnitudes of f_1 and f_2 and their derivatives with respect to α and β can be bounded by some finite constants for all α and β within the level set of V_1 defined by the initial conditions, e.g., $|f_1| \le \kappa_1, x_1, x_2 \in \mathcal{D}_1$. Here, V_1 is the Lyapunov function defined in Eq. (30).

Assumption 8. The magnitude of θ is bounded by some constant less than 90 deg, i.e., $|\theta| \le \theta_m < 90$ deg. The main result of this paper is given next.

Theorem 2. Suppose assumptions 1–8 hold. Then there exist ω_i^* large enough that, for the nonlinear closed-loop system given by Eqs. (15–20), the origin is an exponentially stable equilibrium point.

The remainder of the paper is devoted to proving this result. Some of the details of the proof are omitted, but can be found in Ref. 12.

C. Lyapunov Stability Analysis

The first step in analyzing the stability of Eqs. (15–20) is finding the equilibrium points of the system.

Lemma 3. The origin is the only equilibrium point of Eqs. (15–20).

Proof. To find the equilibrium points of the system we must set Eqs. (15–20) equal to zero. Then Eqs. (15), (17), and (19) require $x_2 = 0$, $x_4 = 0$, and $x_6 = 0$. With $x_2 = 0$ and $x_4 = 0$, Eqs. (16) and (18) require $x_1 = 0$ and $x_3 = 0$. All that is left is to examine Eq. (20). With $x_1 = 0$, $x_3 = 0$, $f_1 = 0$, and $f_2 = 0$ and so Eq. (20) requires $x_5 = 0$. □

1. *Lyapunov Function for α and β*

Next, we will propose a Lyapunov function for the α and β dynamics. This Lyapunov function will later be augmented to include the entire system. Consider the quadratic form

$$V_1 = \tfrac{1}{2}k_1x_1^2 + \tfrac{1}{2}k_2x_2^2 + \tfrac{1}{2}k_3x_3^2 + \tfrac{1}{2}k_4x_4^2 + k_5x_1x_2 + k_6x_3x_4 \tag{30}$$

Clearly, V_1 can be expressed as $V_1 = x^T P_1 x$ with

$$P_1 = \frac{1}{2}\begin{pmatrix} k_1 & k_5 & 0 & 0 \\ k_5 & k_2 & 0 & 0 \\ 0 & 0 & k_3 & k_6 \\ 0 & 0 & k_6 & k_4 \end{pmatrix} \tag{31}$$

Our goal is to find a condition under which $\dot{V}_1$ is negative definite along the trajectory of Eqs. (15–18). Let $k_1 = k_2\omega_i\omega_\alpha + k_5\omega_i$ and $k_3 = k_4\omega_i\omega_\beta + k_6\omega_i$. Taking the derivative of Eq. (30) along the trajectory of Eqs. (15–18) gives

$$\dot{V}_1 = -k_5\omega_i\omega_\alpha x_1^2 + \left(k_5 - k_2\omega_i + k_2\frac{\partial f_1}{\partial \alpha}\right)x_2^2 - k_6\omega_i\omega_\beta x_3^2 + \left(k_6 - k_4\omega_i k_4 + k_4\frac{\partial f_2}{\partial \beta}\right)x_4^2 + x_1x_2k_5\frac{\partial f_1}{\partial \alpha} + x_1x_4k_5\frac{\partial f_1}{\partial \beta} + x_2x_3k_6\frac{\partial f_2}{\partial \alpha} + x_2x_4\left(k_2\frac{\partial f_1}{\partial \beta} + k_4\frac{\partial f_2}{\partial \alpha}\right) + x_3x_4k_6\frac{\partial f_2}{\partial \beta} + (k_5x_1 + k_2x_2)l_1 + (k_6x_3 + k_4x_4)l_2 \tag{32}$$

Equations (21) and (22) imply that

$$|l_1| \le c_{14}|x_4| + c_{124}|x_2x_4| + c_{12}|x_2| + c_{144}\left|x_4^2\right| + c_{146}|x_4x_6| \tag{33}$$

$$|l_2| \le c_{222}\left|x_2^2\right| + c_{22}|x_2| + c_{224}|x_2x_4| + c_{226}|x_2x_6| \tag{34}$$

with $\rho = |1/\det(h)|$, $c_{146} = \rho|\sec^2\beta|$, $c_{12} = \rho|f_2|(|\tan^2\beta\tan\theta| + |\tan\beta\sin\alpha\tan\theta| + |\tan\beta|)$, and the other coefficients are similarly defined, based on Eqs. (21–23). Using these bounds on the size of l_1 and l_2 we find that

$$\dot{V}_1 \le e_{11}x_1^2 + e_{22}x_2^2 + e_{33}x_3^2 + e_{44}x_4^2 + e_{24}|x_2x_4| + e_{12}|x_1x_2| + e_{14}|x_1x_4| + e_{34}|x_3x_4| + e_{23}|x_2x_3| \tag{35}$$

where $e_{11} = -k_5\omega_i\omega_\alpha$, $e_{22} = [k_5 - k_2\omega_i + k_2(\partial f_1/\partial\alpha)] + (k_2c_{124} + k_4c_{222})x_4 + (k_6c_{222})x_3$, $e_{33} = -k_6\omega_i\omega_\beta$, and the other coefficients can be found from Eqs. (32–34). The state x only appears in the e_{ij} terms linearly, with positive coefficients.

Equation (35) can be rewritten as $\dot{V}_1 \le -x^T Q_1 x$ with $x = (x_1, x_2, x_3, x_4)^T$ and

$$Q_1 = -\begin{bmatrix} e_{11} & e_{12}/2 & 0 & e_{14}/2 \\ e_{12}/2 & e_{22} & e_{23}/2 & e_{24}/2 \\ 0 & e_{23}/2 & e_{33} & e_{34}/2 \\ e_{14}/2 & e_{24}/2 & e_{34}/2 & e_{44} \end{bmatrix} \tag{36}$$

The key result of this section can be summarized as follows.

Lemma 4. Suppose Q_1 is positive definite. Then the derivative of the Lyapunov function V_1 along the trajectory of Eqs. (15–18) is negative definite.

Note that Q_1 is a state-dependent matrix, not a constant matrix. The statement that Q_1 is positive definite in a region means that, for all states in that region, there exists an $\epsilon > 0$ such that $Q_1 > \epsilon I$.

2. Lyapunov Analysis for the Complete Dynamics

To perform a Lyapunov stability analysis of the complete dynamics, we augment the Lyapunov function V_1 to include the ϕ dynamics. If we define $V_2 = \frac{1}{2}k_7x_5^2 + \frac{1}{2}k_8x_6^2 + k_9x_5x_6$ then $\dot{V}_2 = -k_9\omega_i\omega_\phi x_5^2 + (k_9 - k_8\omega_i)x_6^2 + (k_9x_5 + k_8x_6)l_3$. Now, examining Eq. (23), we can see that

$$|l_3| \le c_{31}|x_1| + c_{32}|x_2| + c_{33}|x_3| + c_{34}|x_4| + c_{36}|x_6| + c_{326}|x_2x_6| + c_{346}|x_4x_6| + c_{366}|x_6x_6| \tag{37}$$

with $c_{31} = \rho|(\partial f_1/\partial\alpha)\sec^2\theta\dot{\theta}|$, $c_{32} = \rho|\sec^2\theta\dot{\theta}|$, and the other c_{ijk} terms found from Eq. (23) in a manner similar to that used for l_1 and l_2. In bounding l_3, it was necessary to restrict α_c to $\alpha_c = \alpha_1$, where α_1 is the value for which $f_1 = 0$, so that we can say that

$$|\dot{\theta}f_1| \le \left|\dot{\theta}\max\left(\frac{\partial f_1}{\partial\alpha}\right)_{\max}\right||x_1|$$

With these bounds on the size of l_3,

$$\dot{V}_2 \le e_{55}x_5^2 + e_{66}x_6^2 + e_{25}|x_2x_5| + e_{56}|x_5x_6| + e_{45}|x_4x_5| + e_{26}|x_2x_6| + e_{15}|x_1x_5| + e_{35}|x_3x_5| + e_{46}|x_4x_6| + e_{16}|x_1x_6| + e_{36}|x_3x_6| \tag{38}$$

with $e_{55} = -k_9\omega_i\omega_\phi$, $e_{25} = k_9c_{32}$, $e_{26} = k_8c_{32} + k_9c_{326}x_5$, and the other e_{ij} found from Eqs. (37) and (38). Further details can be found in Ref. 12.

With a Lyapunov function for the complete dynamics defined as $V_t = V_1 + V_2$, then $V_t = x^TP_tx$, $\dot{V}_t = \dot{V}_1 + \dot{V}_2$, and $\dot{V}_t \le -x^TQ_tx$ with

$$Q_t = -\begin{pmatrix} e_{11} & e_{12}/2 & 0 & e_{14}/2 & e_{15}/2 & e_{16}/2 \\ e_{12}/2 & e_{22} & e_{23}/2 & e_{24}/2 & e_{25}/2 & e_{26}/2 \\ 0 & e_{23}/2 & e_{33} & e_{34}/2 & e_{35}/2 & e_{36}/2 \\ e_{14}/2 & e_{24}/2 & e_{34}/2 & e_{44} & e_{45}/2 & e_{46}/2 \\ e_{15}/2 & e_{25}/2 & e_{35}/2 & e_{45}/2 & e_{55} & e_{56}/2 \\ e_{16}/2 & e_{26}/2 & e_{36}/2 & e_{46}/2 & e_{56}/2 & e_{66} \end{pmatrix}$$

$$P_t = \frac{1}{2}\begin{pmatrix} k_1 & k_5 & 0 & 0 & 0 & 0 \\ k_5 & k_2 & 0 & 0 & 0 & 0 \\ 0 & 0 & k_3 & k_6 & 0 & 0 \\ 0 & 0 & k_6 & k_4 & 0 & 0 \\ 0 & 0 & 0 & 0 & k_7 & k_9 \\ 0 & 0 & 0 & 0 & k_9 & k_8 \end{pmatrix}$$

As with Q_1 before, Q_t is a state-dependent matrix. In the next section, we will find bounds on the terms in Q_t, enabling us to prove it is positive definite.

Lemma 5. Suppose Q_t is positive definite. Then the derivative of the Lyapunov function V_1 along the trajectory of Eqs. (15–20) is negative definite.

If P_t and Q_t are positive definite near the origin, then the origin is exponentially stable. P_t can be made positive definite by the appropriate choice of k_i. This condition is easily met. To make Q_t positive definite, a large enough ω_i must be chosen. This will be discussed in the succeeding sections.

3. Limits on the Terms in the $\dot{V}$ Equations

To find an ω_i such that $\dot{V}_t$ is negative, many of the terms in Eqs. (21–23) must be finite. In this section, we will discuss bounds on the magnitudes of these terms. Some of the terms, such as f_1 and f_2 and their derivatives are based on the aerodynamic coefficients and their values can be calculated using the aerodynamic data. The largest possible values can be calculated and used as bounds on the magnitudes of these terms. Other terms, such as the magnitudes of x_1, x_2, etc., can be determined using the Lyapunov functions discussed in the preceding section.

State magnitude bounds from level sets. Level sets of the Lyapunov functions V_1 and V_t can be used to bound the magnitudes of $x_1, \ldots, x_6$. If $\dot{V}_1 \le 0$ inside a level set of V_1 defined by the initial condition, then the trajectory of $x_1, \ldots, x_4$ will never leave this set. Similarly, if $\dot{V}_t \le 0$ inside a level set of V_t defined by the initial condition, then the trajectory of $x_1, \ldots, x_6$ will never leave this set. We will later show that $\dot{V}_1 \le 0$ inside this level set of V_1 and that $\dot{V}_t \le 0$ inside this level set of V_t and so the system trajectory stays inside these level sets.

With an initial condition of

$$\begin{aligned} x_1 &= x_{1_0}, & x_2 &= 0, & x_3 &= 0 \\ x_4 &= 0, & x_5 &= x_{5_0}, & x_6 &= 0 \end{aligned} \tag{39}$$

a level set of V_1 is defined by $V_{10} = \frac{1}{2}k_1x_{1_0}^2$. Because V_1 is positive definite, the largest values of x_1 and x_2 in the level set defined by $V_1 = V_{10}$ occur when $x_3 = 0$ and $x_4 = 0$. These values can be found by solving $V_{10} = \frac{1}{2}k_1x_1^2 + \frac{1}{2}k_2x_2^2 + k_5x_1x_2$ for the maximum values of x_1 and x_2 on the level set. For $\omega_i > 1$, this gives

$$|x_1| \le \sqrt{1\Big/\left[1 - \frac{k_5^2}{k_2(k_2\omega_\alpha + k_5)}\right]}\,|x_{1_0}| \tag{40}$$

and

$$|x_2| \le \sqrt{1\Big/\left[1 - \frac{k_5^2}{k_2(k_2\omega_\alpha + k_5)}\right]}\sqrt{\frac{k_2\omega_\alpha + k_5}{k_2}}\,|x_{1_0}|\sqrt{\omega_i} \tag{41}$$

A similar development can be perfomed for x_3 and x_4, giving

$$|x_3| \le \sqrt{1\Big/\left[1 - \frac{k_6^2}{k_4(k_4\omega_\beta + k_6)}\right]}\sqrt{\frac{k_2\omega_\alpha + k_5}{k_4\omega_\beta + k_6}}\,|x_{1_0}| \tag{42}$$

$$|x_4| \le \sqrt{1\Big/\left[1 - \frac{k_6^2}{k_4(k_4\omega_\beta + k_6)}\right]}\sqrt{\frac{k_2\omega_\alpha + k_5}{k_4}}\,|x_{1_0}|\sqrt{\omega_i} \tag{43}$$

Let $\mathcal{D}_1$ be the region defined by Eqs. (40–43). Note that $\mathcal{D}_1$ is not actually a level set of V_1, but rather a hyperbox containing the level set of V_1. It gives us the limits on the values of the individual states inside the level set defined by the initial conditions. This result is summarized in lemma 6.

Lemma 6. Suppose the derivative of V_1 along the trajectory of Eqs. (15–18) is negative definite and the initial condition of the system is given by Eq. (39). Then the trajectory of the states $x_1, \ldots, x_4$ will not leave $\mathcal{D}_1$.

Similarly, a level set of V_t is defined by $V_{t0} = \frac{1}{2}k_1x_{1_0}^2 + \frac{1}{2}k_7x_{5_0}^2$. This level set can be used to determine bounds on x_5 and x_6 that will not be exceeded as long as $\dot{V}_t \le 0$. If we use V_{t0} in the place of V_{10} and perform a similar development for x_5 and x_6, we find that, for $\omega_i \ge 1$,

$$|x_5| \le \sqrt{1\Big/\left[1 - \frac{k_9^2}{k_8(k_8\omega_\phi + k_9)}\right]}\sqrt{x_{5_0}^2 + x_{1_0}^2\frac{k_2\omega_\alpha + k_5}{k_8(k_8\omega_\phi + k_9)}} \tag{44}$$

$$|x_6| \le \sqrt{1\Big/\left[1 - \frac{k_9^2}{k_8(k_8\omega_\phi + k_9)}\right]} \times \sqrt{\frac{x_{1_0}^2(k_2\omega_\alpha + k_5) + x_{5_0}^2(k_8\omega_\phi + k_9)}{k_8}}\sqrt{\omega_i} \tag{45}$$

Let $\mathcal{D}_2$ be the region defined by Eqs. (44) and (45) and let $\mathcal{D}_t$ be the region where $x_1, \ldots, x_4$ are in $\mathcal{D}_1$ and x_5 and x_6 are in $\mathcal{D}_2$. The key result of this development can now be stated in lemma 7.

Lemma 7. Suppose the derivative of V_t along the trajectory of Eqs. (15–20) is negative definite and the initial condition of the system is given by Eq. (39). Also suppose the derivative of V_1 along the trajectory of Eqs. (15–18) is negative definite. Then the trajectory of the states $x_1, \ldots, x_6$ will remain in $\mathcal{D}_t$.

Note that bounds on x_1, x_3, and x_5 also give bounds on α, β, and ϕ.

State magnitude bounds from the inversion equations. To prove that Q_1 and Q_t are negative definite, we also need a bound on the size of $\dot{\theta}$. Such a bound can be found by examining the inversion equations. We can calculate bounds on the sizes of the body rates p, q, and r from the way p_c, q_c, and r_c are generated in the dynamic inversion. These bounds on the body rates can in turn be used to calculate bounds on the sizes of $\dot{\theta}$ and $\dot{\phi}$. This result is summarized in lemma 8.

Lemma 8. Suppose assumptions 6–8 hold. Further suppose that there exist constants $M_1, M_2, M_3 > 0$ such that $\|x_1\| \leq M_1$, $\|x_3\| \leq M_2$, and $\|x_5\| \leq M_3$ and $\det(h)$ is nonsingular within these bounds. Then, the magnitudes of $\dot{\phi}$ and $\dot{\theta}$ are bounded by some positive constants κ_3 and κ_4, which are independent of ω_i.

Proof. First, we note that $\dot{p} = \omega_i(p_c - p)$ and, taking the Laplace transform, $p(s) = \omega_i/(s + \omega_i)p_c(s)$ and, therefore, $\|p\|_\infty \leq \|\omega_i/(s + \omega_i)\|_{L_1}\|p_c\|_\infty = 1 \cdot \|p_c\|_\infty$. The expressions for p_c, q_c, and r_c are given by Eq. (25). Each term in this equation can be bounded, giving bounds on p_c, q_c, and r_c.

Bounds on the magnitudes of f_1 and f_2 can be determined from the aerodynamic data. Bounds on x_1, x_3, and x_5 are given by Eqs. (40), (42), and (44). Bounds on every term in these equations are now available, allowing the calculation of maximum bounds for p, q, and r for whatever size α and ϕ commands are allowed. Once we have bounds on p, q, and r such that $|p| \leq p_m$, $|q| \leq q_m$, and $|r| \leq r_m$, we can bound $\dot{\theta}$. We know $\dot{\theta} = q\cos\phi + r\sin\phi$ and, therefore, $\dot{\theta} \leq 1.414\max(q_m, r_m)$. Also, Eq. (1) can be used to calculate a new upper bound for x_6: $|\dot{\phi}| \leq p_m + q_m|\tan\theta_m| + r_m|\tan\theta_m|$. Further details of these steps can be found in Ref. 12. □

Note that this new upper bound for the magnitude of x_6 does not depend on ω_i. Bounds for x_2 and x_4 can also be calculated in the same manner. However, the bounds on x_2 and x_4 calculated in this manner are generally larger than those found using level sets of V_1 and, therefore, are not practically useful.

4. Proof That Q_1, Q_t Can Be Made Positive Definite

We now have bounds on all of the terms in the expressions for Q_1 and Q_t. We can use these bounds to show that Q_1 and Q_t will be positive definite for large enough ω_i.

Lemma 9. Suppose assumptions 6–8 hold. Then, there exists ω_i^* such that for all $\omega_i \geq \omega_i^*$, Q_1 and Q_t will be positive definite.

Proof. Using the bounds on the states $x_1, \ldots, x_6$ and $\dot{\theta}$ found in Sec. III.C.3, all of the e_{ij} terms in Q_1 and Q_t can be bounded, resulting in matrices that are functions of ω_i only. Each diagonal element has one term that is linear in ω_i with a positive coefficient. All other terms in the matrices are proportional to $\omega_i^{1/2}$ at most.

The matrices Q_1 and Q_t are positive definite if and only if all their leading principal minors have positive determinants. For the leading principal minor corresponding to an $n \times n$ matrix, each element of the determinant is the product of n elements of the matrix. If L_n is the nth leading principal minor of Q_1 or Q_t, then $\det(L_n) = \kappa\omega_i^n + \lambda$ where κ is a positive constant and λ is the rest of the determinant not including the $\kappa\omega_i^n$ term. All other terms in the determinant are proportional to $\omega^{n-1/2}$ at most. Therefore, for some $\omega_i \gg 0$, $\det(L_n) > 0\ \forall n = 1, \ldots, 4$. Therefore, Q_1 is positive definite for all $\omega_i > \omega_i^*$, $\omega_i^* \gg 0$. The proof for Q_t is identical, except n goes up to 6. A different ω_i^* will be found for each matrix. We select the larger of the two values for ω_i^* and the lemma has been proven. □

We have proven that, inside a level set of V_1 defined by the initial condition of the state, $\dot{V}_1$ is negative definite. Therefore, the states $x_1, \ldots, x_4$ do not leave this set. Note that this is only true if x_6 stays less than some bound. But, it has also been proven that, inside a level set of V_t defined by the initial condition of the state and inside the level set of V_1, $\dot{V}_t$ is negative definite. Therefore, the states x_5 and x_6 do not leave this set. This result is summarized in lemma 10.

Lemma 10. Suppose assumptions 6–8 hold. Then for $\omega_i \geq \omega_i^*$, the trajectory of the states $x_1, \ldots, x_6$ will remain within $\mathcal{D}_t$.

For the case where there are nonzero initial conditions only in x_1 and x_5, the bounds on the states are given by Eqs. (41–45). If there were nonzero initial conditions in other states, the new bounds on the states could be calculated from level sets of V_1 and V_t based on the new initial condition.

Proof of Theorem 2. The proof of theorem 2 can now be constructed as follows. First, we showed that the origin is the only equilibrium point of the dynamic system $x_1, \ldots, x_6$. This result is proven as lemma 3. Next, we showed that, if $Q_1 > 0$, then $\dot{V}_1$ is negative definite and if $Q_t > 0$, then $\dot{V}_t$ is negative definite. These results were proven as lemmas 4 and 5. Next, we found bounds on the magnitudes of the state variables, using level sets of the Lyapunov functions V_1 and V_t and the inversion equations. These bounds were given in lemmas 6 and 7. Finally, we have shown that for $\omega_i \geq \omega_i^*$, with ω_i^* large enough, Q_1 and Q_t are positive definite inside the level sets defined by $\mathcal{D}_1$ and $\mathcal{D}_t$. Therefore, for $\omega_i \geq \omega_i^*$, $\dot{V}_1 < 0$ and $\dot{V}_t < 0$ inside $\mathcal{D}_1$ and $\mathcal{D}_t$ and the state trajectory never leaves $\mathcal{D}_t$. This means that the $\dot{V}_t$ is negative definite during the entire motion of the system. Therefore, the system is exponentially stable about the equilibrium point $x_1, \ldots, x_6 = 0$. □

5. Extensions of the Stability Analysis

The stability analysis presented can be extended in a number of ways that are not discussed in detail here due to space constraints. The Lyapunov function V_1 can be used to show that the system is stable about $x_1, \ldots, x_4 = 0$ for any α_c as long as x_6 is bounded, whether the x_5 and x_6 dynamics are stable or not. For maneuvers only involving the longitudinal dynamics (states x_1 and x_2), a simplified Lyapunov function can be used to show the system is exponentially stable about $x_1 = 0$ and $x_2 = 0$ with fewer assumptions.

IV. Numerical Example and Simulation

In this section, a concrete, numerical example is given to illustrate the methodology detailed in the preceding section. This example shows that reasonable bounds on the states can be found from the Lyapunov functions and illustrates how calculations can be done for the various steps in the procedure. Nonlinear simulation results will also be presented as further validation of the controller. The maneuver examined is a step command in α from 5 to 20 deg and in ϕ from 0 to −180 deg, with an initial speed of 1936 ft/s (Mach 2) and an initial altitude of 40,000 ft. The controller attempts to keep β near zero throughout the maneuver.

A. Calculation of State Bounds, Sufficient ω_i^*

We assume that $\theta < \theta_m$ during the maneuver and, in this example, $\theta_m = 24$ deg. The ω and k_i values given in Table 2 are used. These values of ω_α, ω_β, and ω_ϕ were chosen to give good dynamic performance. The values of the k_i were chosen to give useful bounds on the magnitudes of the states.

With these values, V_{10} gives the following bounds on $x_1, \ldots, x_4$: $|x_1| \leq 0.262$ rad, $|x_2| \leq 4.54$ rad/s, $|x_3| \leq 0.117$ rad, and $|x_4| \leq 2.62$ rad/s. Assuming a ϕ command of no more than 180 deg, V_{t0} gives the following bounds on x_5 and x_6: $|x_5| \leq 3.15$ rad and $|x_6| \leq 41.87$ rad/s. If the states remain within these bounds, the simulation data gives bounds for f_1 and f_2 and their derivatives: $f_1 \leq 0.3$, $f_2 \leq 0.04$, $\partial f_1/\partial\alpha \leq 0.65$, $\partial f_1/\partial\beta \leq 0.14$, $\partial f_2/\partial\beta \leq 0.25$, $\partial f_2/\partial\alpha \leq 0.075$. The equations bounding p, q, and r can be used to bound $\dot{\theta}$ and find a new bound for x_6. We find that $\dot{\theta} \leq 6.56$ rad/s and $x_6 \leq 20.28$ rad/s. Some of these rate bounds are large and could perhaps be reduced by determining the maximum body rates achievable with maximum control deflections. Use of lower bounds found in such a manner could reduce the conservatism of the ω_i^* calculation.

The bounds on the states x_2, x_4, and x_6 change slightly for each ω_i, and so the bounds must be recalculated for each ω_i tested. In

Table 2 Desired frequencies and Lyapunov function constants

$\omega_\alpha = 6$	$k_1 = 3{,}005$	$k_4 = 30$	$k_7 = 1{,}755$
$\omega_\beta = 10$	$k_2 = 10$	$k_5 = 0.1$	$k_8 = 10$
$\omega_\phi = 3.5$	$k_3 = 15{,}015$	$k_6 = 0.3$	$k_9 = 0.1$

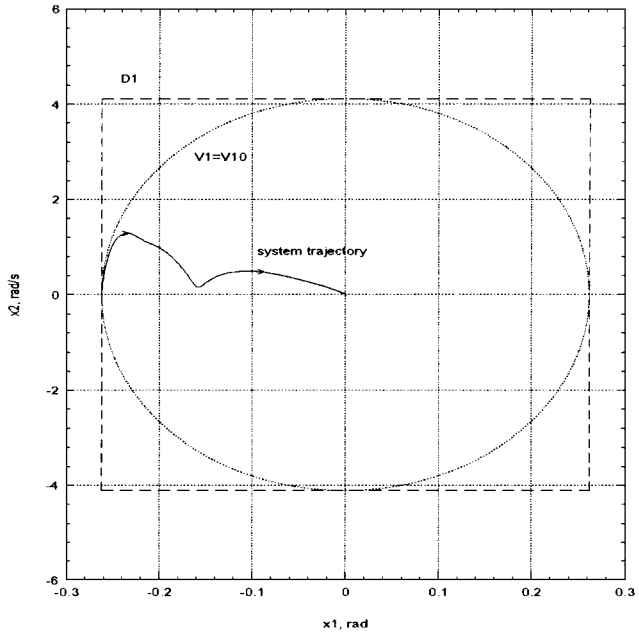

Fig. 2 Trajectory of x_1 and x_2 and bounding sets.

this case, we find that Q_1 is positive definite for $\omega_i \geq 39$ and Q_t is positive definite for $\omega_i \geq 41$. P_1 and P_2 are positive definite for any $\omega_i \geq 1$. If $\omega_i \geq 41$, both $\dot{V}_1$ and $\dot{V}_t$ will be negative definite throughout the motion. This ω_i^* is sufficient to prove stability, but due to the conservatism of the method it is not necessary. The system may also be stable with smaller inner-loop frequencies.

The values of the k_i used in this example were chosen so as to give useful bounds on the states. For example, the controller for a bank-to-turn missile should keep sideslip angle β small. Therefore, we chose k_4 much larger than k_2, allowing us to show that β would not grow larger than 6.71 deg during the maneuver. If a larger k_4 were chosen, a smaller bound on β would be found, but the ω_i needed to guarantee stability would be larger.

In Fig. 2, the projections of $\mathcal{D}_1$ and the level set $V_1 = V_{10}$ into the x_1–x_2 plane are shown, as well as the trajectory of the states x_1 and x_2. The system trajectory starts near the edge of the bounding sets and moves in to the equilibrium at the origin. The origin of the x_1, x_2 system corresponds to $\alpha = \alpha_c$ and $\dot{\alpha} = 0$ in the original system. The simulation results, which are included in this figure, are further discussed in the next section.

B. Simulation Results

The dynamic inversion controller was tested in a six-degree-of-freedom nonlinear missile simulation. The simulation is identical to the one discussed in Refs. 4 and 13, except for the new controller. The simulation contains force and moment look-up tables as functions of Mach number, α, β, control surface deflections, and altitude. The values of ω_α, ω_β, and ω_ϕ used in the example calculations given earlier were used, with $\omega_i = 41$ rad/s.

In the simulation, many of the assumptions used in the derivation of the state-space equations and in the proof of theorem 2 are relaxed. The effects of control deflections on force coefficients were included in the simulation. Acceleration due to gravity was not set to zero. The missile flight speed and dynamic pressure were allowed to vary. Second-order actuator models were included. Finally, we commanded an angle of attack different from the one assumed in the stability analysis. Even with all of these assumptions relaxed, the closed-loop dynamical system with the dynamic inversion controller was stable about $\alpha = \alpha_c$, $\beta = 0$, and $\phi = \phi_c$. The α, β, and ϕ responses are shown in Fig. 3. The α and ϕ responses are approximately first order, as expected. Sideslip angle increases during the period of high roll rate, which is typical of bank-to-turn missiles. The two-tier nature of the α response is due to the high ω_β value making the controller prioritize limiting the growth of sideslip.

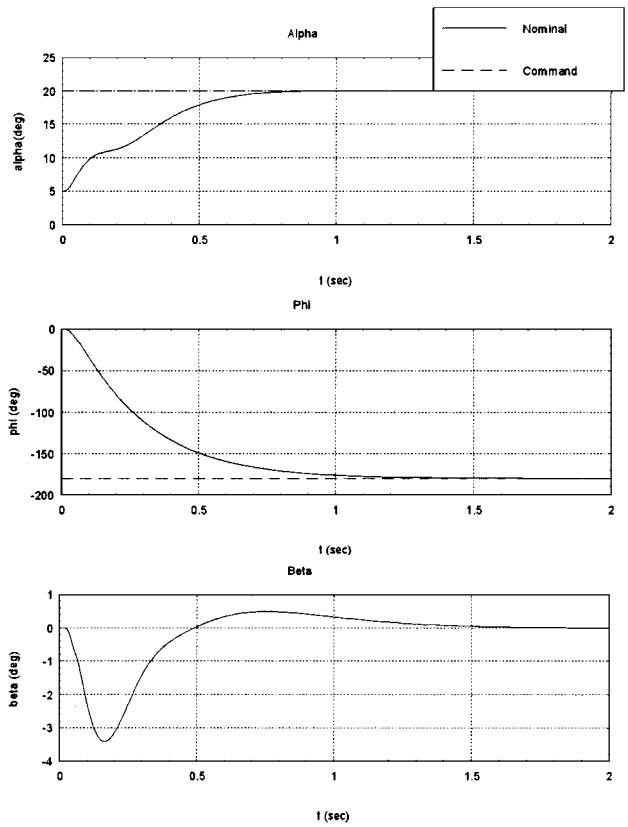

Fig. 3 Closed-loop system response.

V. Conclusions

Results relating to the stability of a bank-to-turn missile system with a dynamic inversion controller were presented. We have derived a state-space representation for the missile dynamics under certain simplifying assumptions. We have shown that, under certain assumptions, the closed-loop stability of the state-space system is guaranteed if the frequency of the desired dynamics in the inner-loop inversion is sufficiently large. An example calculation is included for a bank-to-turn missile, where the inner-loop frequency ω_i^* sufficient to guarantee stability of the missile dynamics is found. Finally, we include the results of a six-degree-of-freedom nonlinear missile simulation with the dynamic inversion controller presented in this paper. This simulation shows that, although the method presented provides a conservative estimate of ω_i^*, not all of the assumptions required in the analysis to prove stability are required for the controller to operate effectively.

Recommendations for future research along the lines presented here include an expansion of the stability result to general α commands and a robustness analysis. The method used in the stability analysis may yield some robustness results for the dynamic inversion controller.

References

[1] Bugajski, D. J., and Enns, D. F., "Nonlinear Control Law with Application to High Angle-of-Attack Flight," *Journal of Guidance, Control, and Dynamics,* Vol. 15, No. 3, 1992, pp. 761–767.

[2] McFarland, M. B., and D'Souza, C. N., "Missile Flight Control with Dynamic Inversion and Structured Singular Value Synthesis," *Proceedings of the AIAA Guidance, Navigation, and Control Conference* (Scottsdale, AZ), AIAA, Washington, DC, 1994, pp. 544–550.

[3] Snell, S. A., Enns, D. F., and Garrard, W. L., "Nonlinear Inversion Flight Control for a Supermaneuverable Aircraft," *Journal of Guidance, Control, and Dynamics*, Vol. 15, No. 4, 1992, pp. 976–984.

[4] Schumacher, C., and Khargonekar, P. P., "A Comparison of Missile Autopilot Designs Using $\mathcal{H}_\infty$ Control with Gain Scheduling and Nonlinear Dynamic Inversion," *Proceedings of the American Control Conference* (Albuquerque, NM), 1997, pp. 2759–2763.

[5] Schumacher, D. A., "Tactical Missile Autopilot Design Using Nonlinear Control," Ph.D. Thesis, Dept. of Aerospace Engineering, Univ. of Michigan, Ann Arbor, MI, 1994.

[6]Hahn, W., *Stability of Motion*, Springer–Verlag, New York, 1967, pp. 102–115, 271–278.

[7]Khalil, H. K., *Nonlinear Systems*, Macmillan, New York, 1992, pp. 97–122, 136–151.

[8]DeSouza, C., and Schumacher, D., "Derivation of the Full Nonlinear Equations of Motion for a Rigid Airframe," *Journal of Guidance, Control, and Dynamics* (to be published).

[9]Blakelock, J. H., *Automatic Control of Aircraft and Missiles*, 2nd ed., Wiley, New York, 1991, Chaps. 1, 7.

[10]Schumacher, C., and Khargonekar, P. P., "Modeling and Control of a Bank-to-Turn Air-to-Air Missile," Dept. of Electrical Engineering and Computer Science, TR CGR97-02, Univ. of Michigan, Ann Arbor, MI, 1997.

[11]Carter, L. H., and Shamma, J. S., "Gain-Scheduled Bank-to-Turn Autopilot Design Using Linear Parameter Varying Transformations," *Journal of Guidance, Control, and Dynamics*, Vol. 19, No. 5, 1996, pp. 1056–1063.

[12]Schumacher, C., "Tactical Missile Autopilots: Gain-Scheduled $\mathcal{H}_\infty$ Control and Dynamic Inversion," Ph.D. Thesis, Dept. of Aerospace Engineering, Univ. of Michigan, Ann Arbor, MI, 1997.

[13]Schumacher, C., and Khargonekar, P. P., "Missile Autopilot Designs Using $\mathcal{H}_\infty$ Control with Gain Scheduling and Nonlinear Dynamic Inversion," *Journal of Guidance, Control, and Dynamics*, Vol. 21, No. 2, 1998, pp. 234–243.